

Echo of the Quantum Phase Transition of $\text{CeCu}_{6-x}\text{Au}_x$ in XPS: Breakdown of Kondo Screening

M. Klein,¹ J. Koha,² H. v. Lohneysen,^{3,4} O. Stockert,⁵ and F. Reinert^{1,6}

¹Universität Würzburg, Experimentelle Physik II, Am Hubland, D-97074 Würzburg, Germany

²Physikalisches Institut and Bethe Center for Theoretical Physics,
Universität Bonn, Nussallee 12, D-53115 Bonn, Germany

³Physikalisches Institut, Universität Karlsruhe (TH), D-76128 Karlsruhe, Germany

⁴Forschungszentrum Karlsruhe, Institut für Festkörperphysik, D-76021 Karlsruhe, Germany

⁵Max Planck Institute for Chemical Physics of Solids, Nothnitzer Str. 40, 01187 Dresden, Germany

⁶Forschungszentrum Karlsruhe, Gemeinschaftslabor für Nanoanalytik, D-76021 Karlsruhe, Germany
(Dated: February 21, 2024)

We present an X-ray photoemission study of the heavy fermion system $\text{CeCu}_{6-x}\text{Au}_x$ across the magnetic quantum phase transition of this compound at temperatures above the single-ion Kondo temperature T_K . In dependence of the Au concentration x we observe a sudden change of the f -occupation number n_f and the core-hole potential U_{cf} at the critical concentration $x_c = 0.1$. We interpret these findings in the framework of the single-impurity Anderson model. Our results are in excellent agreement with findings from earlier UPS measurements and provide further information about the precursors of quantum criticality at elevated temperatures.

PACS numbers: 71.27.+a, 71.28.+d, 79.60.-i, 71.10.-w

I. INTRODUCTION

$\text{CeCu}_{6-x}\text{Au}_x$ is one of the best characterized heavy-fermion (HF) compounds^{1,2,3,4,5} exhibiting a quantum phase transition (QPT) between a paramagnetic phase with full Kondo screening of the Ce $4f$ moments and an antiferromagnetic phase induced by their RKKY coupling.⁶ The QPT occurs at a critical Au concentration of $x = x_c = 0.1$. Two major scenarios for the QPT have been put forward, firstly the Hertz-Millis scenario^{7,8} where only the (bosonic) magnetic fluctuations become critical, leaving the (fermionic) heavy quasiparticles intact, and secondly the local quantum criticality^{9,10} where the local Kondo quasiparticles are destroyed by coupling to the quantum critical magnetic fluctuations. In the latter case the Kondo screening scale, or Kondo temperature of the lattice system, T_K , vanishes at the quantum critical point (QCP). Despite intense efforts it has not been possible to unambiguously identify either one scenario in $\text{CeCu}_{6-x}\text{Au}_x$. The difficulty resides in the fact that near the QCP many different effects come into play, including local Kondo screening, lattice coherence and Fermi volume collapse, quantum critical fluctuations, and possible dimensional reduction.^{2,11} They have prevented a conclusive experimental picture as well as a unified theory of the QPT. Recently we have presented direct measurements of the evolution of the local Kondo screening energy scale T_K across the QCP as extracted from high-resolution ultraviolet photoemission spectroscopy (UPS).¹² Taking impurity spectra clearly above T_K as well as above the lattice coherence temperature T_{coh} and the Neel temperature for magnetic ordering, T_N ($T > \text{fT}_K; T_{\text{coh}}; T_N$), made it possible to probe the local energy scale without the complications caused by lattice coherence or quantum critical fluctuations. The surprising outcome of these investigations is that the precursors of the QPT are already

visible in the single-impurity T_K as extracted from UPS spectra at such elevated temperatures. In Ref. [12] we developed a theory, based on the effective single-impurity model realized for temperatures $T > T_{\text{coh}}$, where the Kondo exchange coupling J of a Ce site is selfconsistently renormalized by the surrounding, identical Ce atoms only through the indirect RKKY coupling. The theory explains the observed, nontrivial, step-like behavior of T_K near the QCP and supports the local critical scenario for $\text{CeCu}_{6-x}\text{Au}_x$. It also provides a general criterion to distinguish experimentally whether a given HF compound should exhibit HM or local quantum critical behaviour.¹²

UPS provides the most direct access to the screening scale T_K by directly recording the Kondo resonance in the local Ce $4f$ spectrum,^{13,14} but probes a relatively shallow surface region only. Therefore we complement here the studies of Ref. [12] with bulk-sensitive X-ray photoemission spectroscopy (XPS) on the same samples and under the same experimental conditions, even though XPS provides only rather indirect information about the Ce $4f$ spectrum and the physics near the Fermi energy E_F .^{15,16} We find that the XPS results are in full agreement with the UPS analysis.

II. SIGNIFICANCE OF CORE-HOLE SPECTRA

Before we show the experimental results, we briefly recall the energetics of the photoionization process, in order to understand the essential structure of the XPS spectra. In XPS the Ce $3d$ spectrum is recorded in the final state of the Ce ion after creation of a $3d$ core hole. The binding energy of a $3d$ electron is influenced by the electrostatic attraction U_{cf} between the $3d$ core hole and a $4f$ electron and, hence, depends on the number of electrons n in the $4f$ shell. Therefore, the $3d$ peak of the XPS spec-

trum is split into individual resonances, each one corresponding to a different charge state of the 4f shell, the so-called f^n resonances, with $n = 0; 1; 2$. In addition, there is a Coulomb repulsion U_{ff} between two electrons in the 4f shell. The peak position (binding energy $E_B^{(n)}$) of the f^n resonance is the energy difference between the charge configuration in the photoionized state and in the groundstate. Hence, it is roughly given by, up to conduction electron screening corrections,

$$E_B^{(n)} = E_B^{(0)} - n U_{df} + \frac{1}{2} (n^2 - n) U_{ff} : \quad (1)$$

Note that the attractive core hole potential U_{df} changes the whole level scheme.¹⁷ In particular, in the photoionized state the $4f^2$ configuration becomes occupied (see Fig. 1), even though in the Ce groundstate it is shifted far above the Fermi energy by the repulsion U_{ff} . The quantitative ratio of U_{df} and U_{ff} (see below) shows that the binding energy of the $4f^0$ configuration, $E_B^{(0)}$, is the largest. The spectral weight of the f^0 XPS peak is proportional to the Kondo resonance of the Ce 4f spectrum, since in $\text{CeCu}_6-x\text{Au}_x$ most of the Kondo peak weight is located above E_F ¹³ and thus represents the unoccupied configuration of the 4f shell.

III. EXPERIMENTAL RESULTS

All the measurements were carried out at $T = 15$ K and thus at temperatures far above any long-range or quantum critical fluctuations. The experimental setup is equipped with a SCIENTA R4000 analyser and a monochromatized X-ray source (Al K line: X-ray energy $h\nu = 1486$ eV). The pressure in the UHV chamber was $1 \cdot 10^{10}$ mbar. Because of the low intensity due to the small surface area of the crystals and the rapid deterioration of the surface, the instrumental resolution was set to

2 eV in order to optimize the count rate. The investigated samples were single crystals grown in a W crucible under high-purity Ar atmosphere¹⁸ and cleaved in situ at the sample position just before the measurement.

The Ce 3d core-level spectra for all measured compounds are shown in Fig. 1. Taking the second derivative of each spectrum reveals that each of the broad peaks is actually comprised of two resonances. Hence, each spectrum consists of a group of three resonances, termed f^0 , f^1 , and f^2 in Fig. 1. They are, in addition, duplicated due to a spin-orbit splitting of $\Delta_{so} = 18.9$ eV. A rough analysis already shows that the XPS 3d spectra can be divided into two classes, namely for $x = 0.1$ and $x = 0.2$, respectively, like in the case of the UPS 4f spectra.¹² For $x = 0.1$ the f^0 peak at $E_B = 917$ eV is clearly visible, albeit comparatively weak, while for $x = 0.2$ the f^0 weight is almost not discernible and vanishes completely for $x = 1$. In addition, for $x = 0.2$ the f^1 and f^2 peaks are shifted by a constant amount of 1.8 eV towards smaller binding energy relative to their positions for $x = 0.1$.

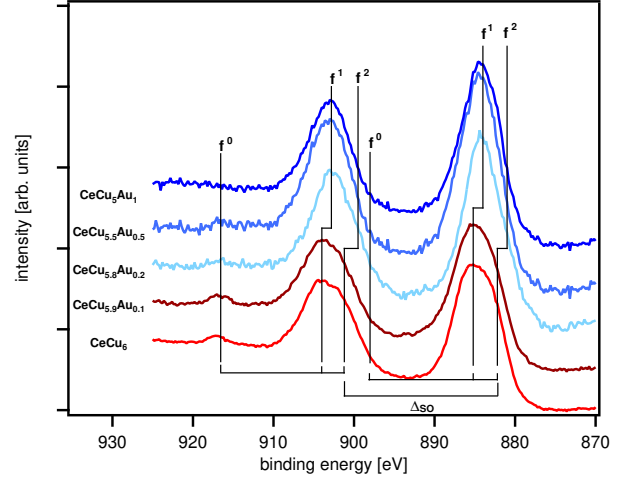


FIG. 1: (color online) 3d core-level spectra of $\text{CeCu}_6-x\text{Au}_x$ for various Au concentrations at $T = 15$ K (X-ray energy $h\nu = 1486$ eV, experimental resolution $\Gamma = 2$ eV). The vertical lines mark the peak positions exhibiting an abrupt shift of the f^1 and f^2 resonances from $x = 0.1$ to $x = 0.2$.

IV. DISCUSSION

In order to interpret these XPS results quantitatively, we calculated the Ce 3d spectra using the Gunnarsson-Schönhammer (GS) theory,^{19,20} which is based on the single-impurity Anderson model (SIAM). From earlier UPS experiments it is known^{12,13,21} that the $\text{CeCu}_6-x\text{Au}_x$ 4f spectra and their T dependence are very well described in the framework of this model for elevated temperatures $T > T_K$, with an RKKY-induced renormalization of the local Kondo coupling.¹² Moreover, the GS theory has been successfully applied to interpret XPS, X-ray photoabsorption, inverse photoemission and valence photoemission spectroscopy on other Ce-based compounds, using the same parameter set for all measurements,^{22,23} albeit small adjustments of parameter values were pointed out to be necessary in some cases.^{24,25} In our GS calculations for $\text{CeCu}_6-x\text{Au}_x$ we use, without fitting, the same parameter values of the SIAM that were determined earlier from noncrossing approximation (NCA) calculations of the UPS 4f spectra of the same compounds.¹² That is, the conduction band half width and the bare 4f level are $D = 2.8$ eV and $\epsilon_f = -1.05$ eV, respectively. The 4f-level hybridization had been determined as $V = 116$ meV for $x = 0.1$ and $V = 108$ meV for $x = 0.2$, corresponding to a reduction of the effective spin exchange coupling $J = 2[\epsilon_f(\epsilon_f + 1) + (\epsilon_f + U_{ff})]$. The XPS 3d spectra involve the additional interaction parameters U_{df} and U_{ff} , see above. Since the intra-4f-level repulsion U_{ff} will not significantly depend on the Au concentration x , we have chosen a constant value of $U_{ff} = 10.0$ eV (within NCA it was assumed to be infinite for simplicity, in order to suppress 4f double occupancy). This leaves the

core hole potential U_{cf} as the only adjustable parameter. It determines the final-state energy levels and thus the position of the core-level peaks relative to each other according to Eq. (1). To fit the theoretical spectra to the experimental results we added to the GS spectra a background, accounting phenomenologically for inelastic scattering of the electrons during the XPS process, and convoluted the theoretical spectra with a Gaussian, accounting for the experimental resolution. This yields $U_{\text{cf}} = 12.5$ eV for $x = 0.1$ and $U_{\text{cf}} = 13.5$ eV for $x = 0.2$. Fig. 2 shows the GS spectra, fitted to the experimental data, and the lower panel of Fig. 3 shows a comparison of the unbroadened GS spectra below and above x_c . The agreement between theory and experiment is remarkable: Both, the relative peak intensities and the shape of the spectra are well reproduced by only a single parameter.

This allows for a detailed interpretation of the experimental data. A reduction of ϵ leads to a significant change in the relative weights of the peaks, as already shown by Gunnarsson and Schonhammer in Refs. [19,20]: For $\epsilon = 108$ meV the f^2 -peak is dim-

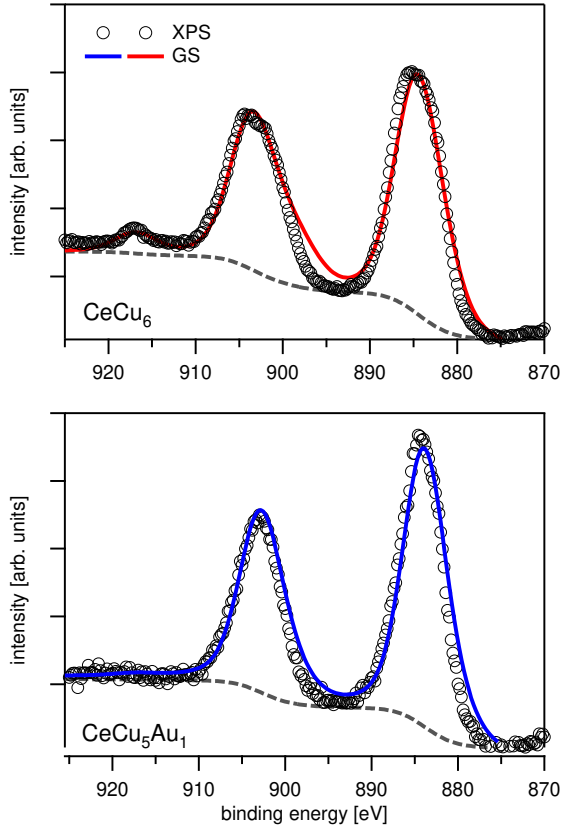


FIG. 2: (color online) Comparison of the experimental XPS data and the theoretical spectra calculated from the GS theory.^{19,20} The dashed lines represent the inelastic background that was added phenomenologically to the theoretical spectra.

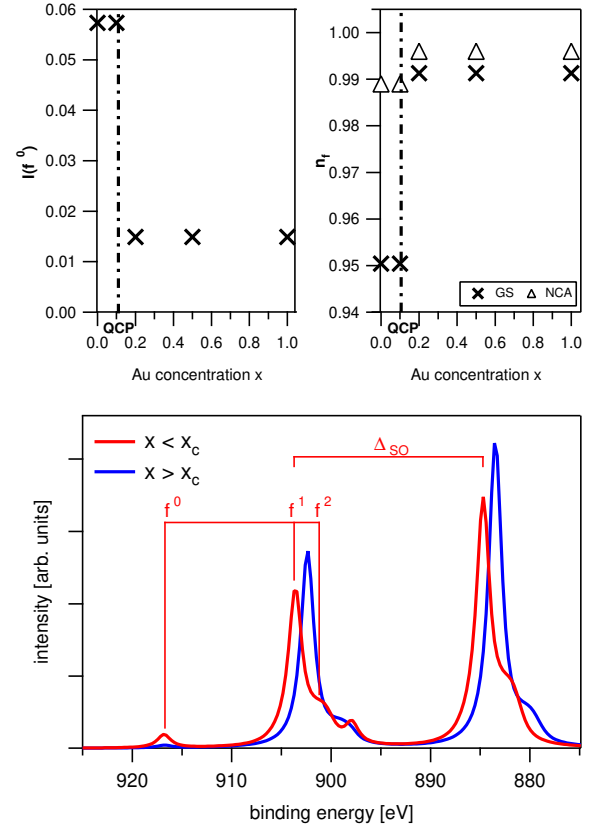


FIG. 3: (color online) The upper left panel shows the weight of the f^0 -configuration as determined from the GS fit. It represents a measure of the weight of the Kondo-resonance in the 4f spectrum (see text). The upper right panel shows the 4f-occupation numbers. In the lower panel the calculated, unbroadened GS spectra are shown for $\text{CeCu}_{6-x}\text{Au}_x$ compounds below and above the quantum critical concentration x_c . The parameter values used in the calculations are given in the text. The vertical lines mark the f^0 , f^1 , f^2 peaks and the SO-shifting for $x < x_c$.

ished and the f^0 -peak has almost vanished. Since the weight of the f^0 -configuration is a measure of the weight of the Kondo resonance (see above), this means for the present $\text{CeCu}_{6-x}\text{Au}_x$ system that the spectral weight of the Kondo resonance drops abruptly as x is changed from $x = x_c$ to $x > x_c$, in full agreement with the findings of UPS in Ref. [12]. In the left upper panel of Fig. 3 we show the weight of the f^0 -configuration as extracted from the GS calculations for different x . It shows a significant step at $x = x_c$. As a consequence of this collapse of the Kondo resonance in the 4f spectrum above the Fermi level, one expects that the spectral weight below E_F and, hence, the f -level occupation number n_f are increased for $x > x_c$ by roughly the Kondo spectral weight. As an immediate, further consequence the 3d electron binding energy should decrease, because the enhancement of n_f increases the attractive interaction exerted by the 4f electrons on the 3d core hole.

Both expectations can be checked from the XPS spectra. Firstly, the decrease of 3d binding energy is indeed seen in the experimental spectra (Fig. 1) and in the fitted theoretical spectra (Fig. 3, lower panel) as the upward shift of the f^1 and f^2 peaks for $x \geq 0.2$ as compared to $x \leq 0.1$. It is also reflected by the increase of the fitted values of the effective core level potential U_{eff} . Secondly, the probability for the 4f occupancy in the groundstate can be extracted from the XPS spectra.^{15,16} It is roughly given by

$$n_f = 1 - \frac{I(f^0)}{I(f^0) + I(f^1) + 2I(f^2)}; \quad (2)$$

where $I(f^n)$ is the (unnormalized) spectral weight of the f^n peak, $n = 0; 1; 2$, after subtraction of the inelastic background. Determining n_f directly from the experimental data is not accurate, since the f^n -peaks overlap and the determination of the inelastic background of the experimental spectra is not trivial. Instead we extract the n_f -numbers from the fitted GS calculations. These include also small deviations from Eq. (2) which arise from the dynamics of the XPS process.^{20,22} In the right upper panel of Fig. 3 we compare the n_f values obtained from the GS calculations and from NCA calculations of Ref. 12. Since n_f increases with temperature,²⁶ it is important to note that the NCA values have been calculated at the experimental temperature of $T = 15$ K. Although the absolute values of n_f differ for the two calculations (probably due to the use of a finite U_{eff} within NCA) the main features are the same: both data sets exhibit a significant, abrupt step of n_f at the critical concentration x_c for the QPT in $\text{CeCu}_{6-x}\text{Au}_x$, as expected from the Kondo resonance collapse observed for $x > 0.1$.

V. CONCLUSION

We have presented data from XPS measurements at elevated temperature on $\text{CeCu}_{6-x}\text{Au}_x$ compounds with

different Au concentrations x across the critical concentration $x_c = 0.1$ of the magnetic quantum phase transition. With increasing x the 3d core spectra exhibit near $x = x_c$ an abrupt change with respect to three different features, namely (1) a collapse of the f^0 resonance, signalling a sudden decrease of Kondo screening, (2) a step-like increase of the 4f occupation number and (3) a sudden increase of the core hole attraction, evidenced by a shift of the f^1 and f^2 peaks towards smaller binding energy. The first feature is in complete agreement with findings of direct UPS measurements of the Kondo resonance in the Ce 4f spectrum. The features (2) and (3) are explained in a natural way as direct consequences of the Kondo resonance collapse. Therefore, the present measurements strongly support that the Kondo resonance collapse observed at the QPT by UPS¹² is not a surface effect but an effect of the bulk $\text{CeCu}_{6-x}\text{Au}_x$ compounds, since it is seen by the bulk-sensitive XPS as well. The analysis of the spectra using the Gunnarsson-Schönhammer theory^{19,20}, supported by NCA calculations, further indicates that the spectra taken at temperatures above the single-impurity Kondo temperature T_K and above the lattice coherence and Neel temperatures T_{coh} , T_N are well described by the single-impurity Anderson model, with the spin exchange coupling J renormalized only by RKKY interactions with the surrounding Ce impurity moments.¹² Thus, our results indicate experimentally that the HM model^{7,8} is insufficient to describe the QPT in $\text{CeCu}_{6-x}\text{Au}_x$ and that at the lowest temperatures the system should follow the local quantum critical scenario,^{9,10} as argued in detail in Ref. 12.

We would like to thank O. Gunnarsson for fruitful discussions and for the allocation of his code. This work was supported by the Deutsche Forschungsgemeinschaft through grant No. Re 1469/4-3/4 (M.K., F.R.), FOR 960 (H.v.L.), and SFB 608 (J.K.).

- ¹ H. v. Lohneysen, A. Schröder, and O. Stockert, *J. Alloys Compd.* 303(304), 480 (2000).
- ² O. Stockert, H. v. Lohneysen, A. Rosch, N. Pyka, and M. Loewenhaupt, *Phys. Rev. Lett.* 80, 5627 (1998).
- ³ A. Schröder, G. Aeppli, R. Coldea, M. Adams, O. Stockert, H. v. Lohneysen, E. Bucher, R. Ramazashvili, and P. Coleman, *Nature* 407, 351 (2000).
- ⁴ H. v. Lohneysen, A. Neubert, T. Pietrus, A. Schröder, O. Stockert, U. Tutsch, M. Loewenhaupt, A. Rosch, and P. Wölle, *Eur. Phys. J. B* 5, 447 (1998).
- ⁵ H. v. Lohneysen, H. Bartolf, S. Drotziger, C. Peiderer, O. Stockert, D. Souptel, W. Loser, and G. Behr, *J. Alloys Compd.* 408(412), 9 (2006).
- ⁶ P. Gegenwart, Q. Si, and F. Steglich, *Nature Phys.* 4, 186 (2008).
- ⁷ J. A. Hertz, *Phys. Rev. B* 14, 1165 (1976).

- ⁸ A. J. Millis, *Phys. Rev. B* 48, 7183 (1993).
- ⁹ Q. Si, S. Rabello, and J. L. Smith, *Nature* 413, 804 (2001).
- ¹⁰ P. Coleman, C. Pepin, Q. Si, and R. Ramazashvili, *J. Phys.: Condens. Matter* 13, 723 (2001).
- ¹¹ A. Rosch, A. Schröder, O. Stockert, and H. v. Lohneysen, *Phys. Rev. Lett.* 79, 159 (1997).
- ¹² M. Klein, A. Nuber, F. Reinert, J. Kroha, and H. v. Lohneysen, *Phys. Rev. Lett.* 101, 266404 (2008).
- ¹³ D. Ehm, S. Hufner, F. Reinert, J. Kroha, P. Wölle, O. Stockert, C. Geibel, and H. v. Lohneysen, *Phys. Rev. B* 76, 045117 (2007).
- ¹⁴ J. W. Allen, *J. Phys. Soc. Jpn.* 74, 34 (2005).
- ¹⁵ F. Reinert, R. Claessen, G. Nicolay, D. Ehm, S. Hufner, W. P. Ellis, G. H. Gweon, J. W. Allen, B. K. Indler, and W. A. M. J. van der Laan, *Phys. Rev. B* 63, 197102 (2001).
- ¹⁶ S. Schmidt, N. Weber, H. J. Elmers, F. Forster, F. Rein-

- ert, S. Hufner, M. Escher, M. Merkel, B. Kromker, and D. Funkenann, *Phys. Rev. B* **72**, 064429 (2005).
- ¹⁷ S. Hufner, *Photoelectron Spectroscopy* (Springer-Verlag, Berlin/Heidelberg/New York, 1994).
- ¹⁸ K. Grube, W. H. Fietz, U. Tutsch, O. Stockert, and H. v. Lohneysen, *Phys. Rev. B* **60**, 11947 (1999).
- ¹⁹ O. Gunnarsson and K. Schonhammer, *Phys. Rev. B* **28**, 4315 (1983).
- ²⁰ O. Gunnarsson, K. Schonhammer, J. C. Fuggle, F. U. Hillebrecht, J. M. Esteve, R. C. Kamatak, and B. Hillebrand, *Phys. Rev. B* **28**, 7330 (1983).
- ²¹ D. Ehm, F. Reinert, G. Nicolay, S. Schmidt, S. Hufner, R. Claessen, V. Eyert, and C. Geibel, *Phys. Rev. B* **64**, 235104 (2001).
- ²² J. C. Fuggle, F. U. Hillebrecht, Z. Zolnierak, R. Lasser, C. Freiburg, O. Gunnarsson, and K. Schonhammer, *Phys. Rev. B* **27**, 7330 (1983).
- ²³ J. W. Allen, S. J. Oh, O. Gunnarsson, K. Schonhammer, M. B. Maple, M. S. Torikachvili, and I. Lindau, *Adv. in Phys.* **35**, 275 (1986).
- ²⁴ N. Witkowski, F. Bertran, and D. M. Alterre, *Phys. Rev. B* **56**, 15040 (1997).
- ²⁵ N. Witkowski, F. Bertran, and D. M. Alterre, *J. Electron Spectrosc. Relat. Phenom.* **117** (2001).
- ²⁶ N. E. Bickers, D. L. Cox, and J. W. Wilkins, *Phys. Rev. B* **36**, 2036 (1987).